Available online at www.sciencedirect.com
ScienceDirect
Journal of Sound and Vibration 325 (2009) 252–265
JOURNAL OF SOUND AND VIBRATION
www.elsevier.com/locate/jsvi

Forced response of light weight plates with truss-like cores

Torsten Kohrs*, Björn A.T. Petersson

Institute of Fluid Mechanics and Engineering Acoustics, Technische Universität Berlin, Einsteinufer 25, 10587 Berlin, Germany

Received 22 September 2008; received in revised form 21 February 2009; accepted 17 March 2009
Handling Editor: C.L. Morfey
Available online 24 April 2009

Abstract

The waveguide finite element (WFE) method is used for forced response calculations of light weight plates with truss-like cores and produces favourable results for plate investigations where the lateral direction is finite. Standard FE-packages can be used to gain the mass and stiffness matrices of a small slice of the plate. The forced response results presented illustrate the strength of the WFE-calculations. This is demonstrated through comparisons with the outcome of standard FE-calculations. The fact that the plate can be taken as infinite in the longitudinal direction without enlarging the computational effort, is especially valuable for general profile design, since otherwise longitudinal resonances would obscure the trends for arbitrary lengths. It is demonstrated that the application of a reduced wave basis can serve as a promising way to limit the necessary calculation effort for WFE-applications. Only if nearfield effects are of primary concern, the full wave basis has to be retained. The application of standard reduction methods like the Guyan or improved reduction system (IRS) is far less reliable and should be avoided.

An example, a regional train floor, demonstrates the applicability of the WFE-method for forced wave propagation on real extruded profile plates. It is demonstrated by mobility measurements that the salient physical behaviour is adequately described by the calculation model.

1. Introduction

The free wave propagation of light weight plates with truss-like cores is investigated thoroughly in Ref. [1] and forms the basis for the forced response calculations in this paper. The calculations are based on the waveguide finite element (WFE) method [2,3]. In contrast to the simplified two-dimensional forced response investigations presented in Ref. [4], which are based on wave propagation in beams, a full three-dimensional investigation is performed in this paper. For structure-borne sound problems where the structure-borne input power from source to the receiving structure is imparted through contacts, which are smaller than the governing wavelengths, the connections can be treated as point contacts. This point force excitation investigated in benchmarked through a comparison of the WFE forced response with the results of a standard FE-calculation for a section of a light weight plate. The calculation effort can be decreased by the application of reduction methods like the Guyan reduction. The influence of such reductions on the input and transfer

*Corresponding author.
E-mail address: torsten.kohrs@de.transport.bombardier.com (T. Kohrs).

0022-460X/$ - see front matter © 2009 Elsevier Ltd. All rights reserved.
doi:10.1016/j.jsv.2009.03.020

mobilities is investigated. Finally, a train floor section is used to validate the method by comparing measured and calculated input mobilities.

2. Theory

Forced response calculations for light weight plates of finite width (x-direction in Fig. 1) can be performed using the wave basis extracted, as outlined in Ref. [1] for the WFE. For finite systems a global dynamic stiffness matrix containing the DOFs at the front and back ends, can be defined and solved as shown in Ref. [5]. For infinite waveguide systems, which are treated in this work, the forced response can be calculated as outlined in Refs. [3,6]. For the systems investigated here it is favourable from a computational point of view to include only the most important (propagating) waves in the forced response calculations. The eigenvalue problem can then be solved only for propagating and slightly decaying waves as discussed in Ref. [6].

The wave amplitude vector $\mathbf{R}$ of the forward (positive z-direction) travelling waves can be calculated with the reduced wave basis for an infinite waveguide system by means of

$$\mathbf{R} = -\mathbf{\Psi}_{\xi}^{+}\mathbf{F_0}. \tag{1}$$

Therein $\mathbf{F_0}$ is the external force/moment excitation vector in the excited slice and $\mathbf{\Psi}_{\xi}^{+}$ is the matrix containing the displacement components for forward travelling waves ($|\lambda_i|<1$) of the *left* eigenvector matrix $\mathbf{\Psi}$. The individual left eigenvectors can be deduced from the right displacement eigenvectors using

$$\boldsymbol{\psi}_i = \frac{1}{d_i}[\boldsymbol{\phi}(1/\lambda_i)_{\xi,i}^{T}(\mathbf{K}_{bb} + \lambda_i\mathbf{K}_{fb}) \quad \boldsymbol{\phi}(1/\lambda_i)_{\xi,i}^{T}]. \tag{2}$$

$\mathbf{K}_{bb}$ and $\mathbf{K}_{fb}$ are sub-matrices of the full dynamic stiffness matrix $\mathbf{K}$ containing only back (bb) and front to back (fb) components respectively, see Ref. [1] for details. The eigenvectors are normalized in Eq. (2) with d_i which is defined as $d_i = \boldsymbol{\psi}_i\boldsymbol{\phi}_i$.

By summing up the contributions of all characteristic waves, the displacements are obtained for the excited slice. The response along the chain of elements can then be calculated from the wave amplitudes at the excitation position [5].

3. Numerical results

Forced response calculations are performed with the theory summarized in the preceding section. In order to benchmark the method and its implementation, a comparison is made with standard FE-calculated results. The infinite extension in the z-direction is approximated by a section of 2 m in the standard FE-calculation with increasing loss factor in the z-direction towards the edge ($\eta = 0.05, \ldots, 0.1$). This boundary condition of about 0.5 m depth is not expected to be perfectly non-reflecting, but will reveal the general trends. A real infinite extension in the z-direction is not feasible in standard FE-calculations and a bigger extension in the z-direction would increase calculation time prohibitively. The WFE-model and the full standard FE-model are depicted in Fig. 1, where the length of the shell elements is 10 mm in both models.

Benchmark results from the comparison of standard FE-result and WFE-result are shown in Figs. 2–5 for the point of excitation and some selected points along the extension in the z-direction.

The differences between the standard FE-results and the WFE-results reduce with increasing frequency. This is expected as the simulated non-reflective boundaries are not efficient at low frequencies, where the damped section is far too small. It is expected that the damped boundary is effective when the wavelengths are shorter than its extension. The frequency where the wavelength equals 0.5 m ($k = 12.6\,\mathrm{m}^{-1}$), the length of the absorbing section, can be extracted from the dispersion plot in Fig. 11. This is roughly 1200 Hz for the first group of local waves cutting on. Hence, reflections leading to additional resonances are expected below this frequency. At higher frequencies, the deviations are strongly reduced.

The results demonstrate the applicability and reliability of the WFE-calculations for the forced response. Tendencies for general structural-acoustic design of the profiles are emphasized in the mobility results, which are independent of the profile length. This is due to the fact that the mean, infinite behaviour is gained in the z-direction, where probably misleading effects of resonances in this direction are suppressed.

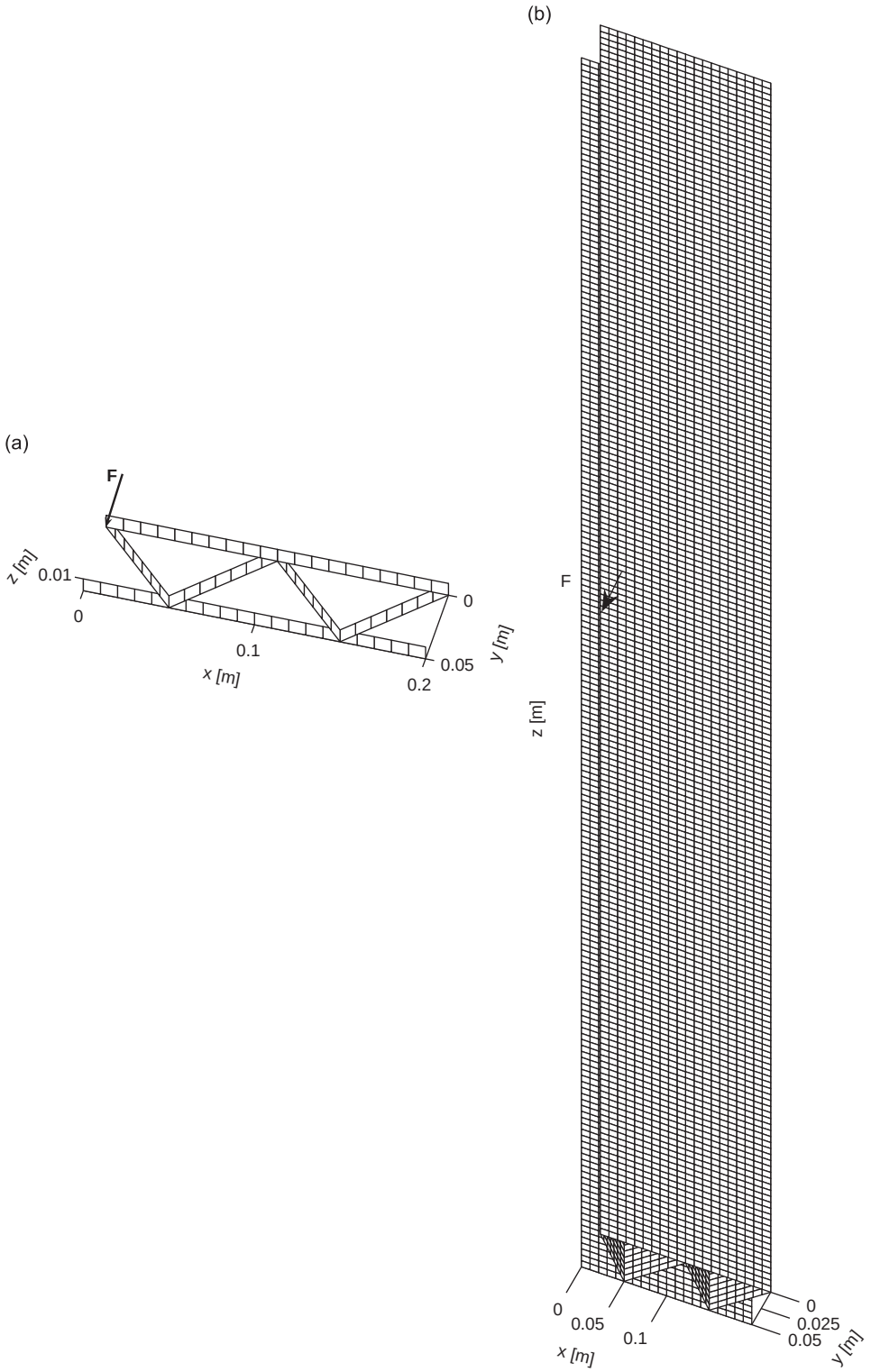

Fig. 1. Models for forced response calculations (two profile A subelements), 10 mm mesh, (a) WFE-model. (b) Standard FE-model.

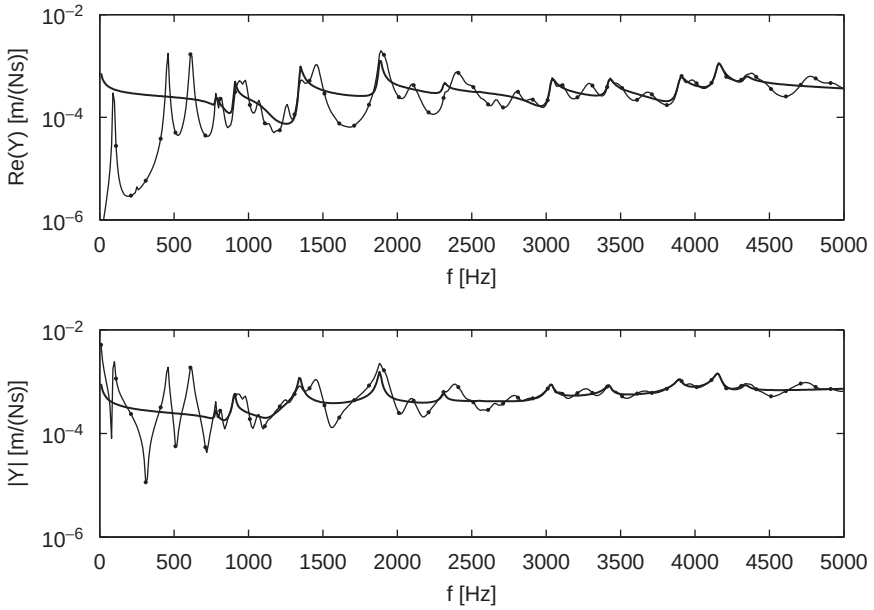

Fig. 2. Input mobility profile A, two subelements, free boundary: standard FE-results -•- and WFE-results –(bold).

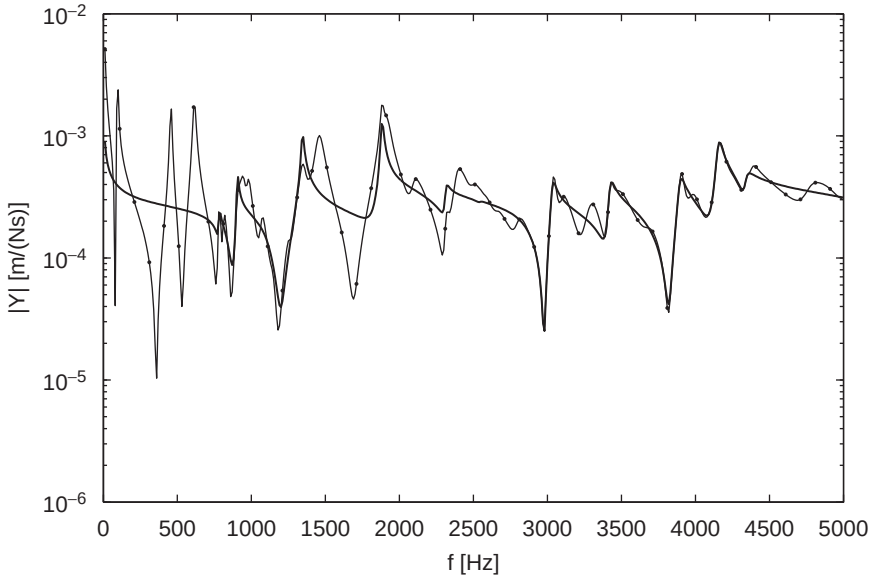

Fig. 3. Transfer mobility profile A, two subelements, free boundary: standard FE-results -•- and WFE-results –(bold) (resp. at $x = 0$, $y = 0$, $z = 0.1$ m).

4. Forced response with reduced wave basis

As shown by Waki et al. [6], the forced response can be calculated with a reduced wave basis by limiting the solution to the principal propagating characteristic waves. Calculation time and memory usage can be significantly reduced by this approach as only a limited number of eigensolutions with $|\lambda| \approx 1$ have to be calculated and stored. This reduced wave basis can then be used for forced response calculations with arbitrary

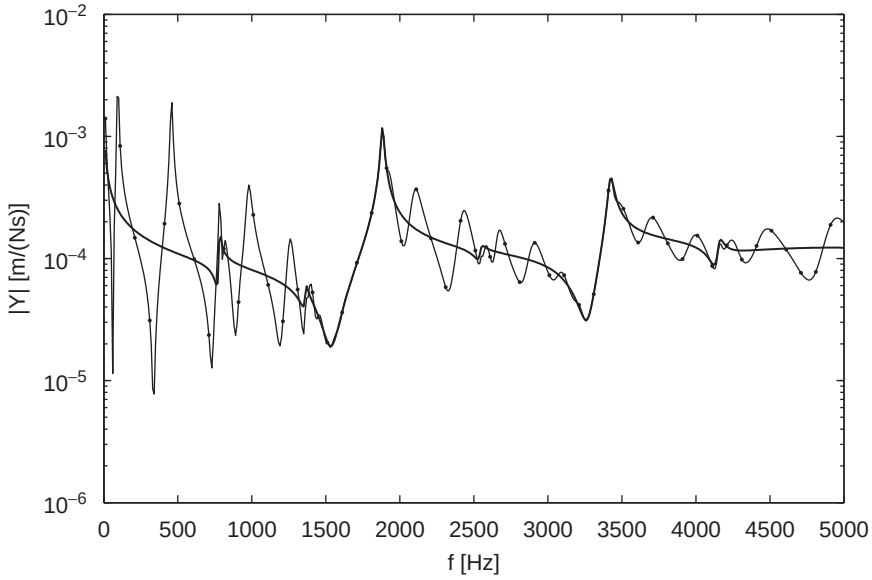

Fig. 4. Transfer mobility profile A, two subelements, free boundary: standard FE-results -•- and WFE-results –(bold) (resp. at $x = 0.1$ m, $y = 0$, $z = 0$).

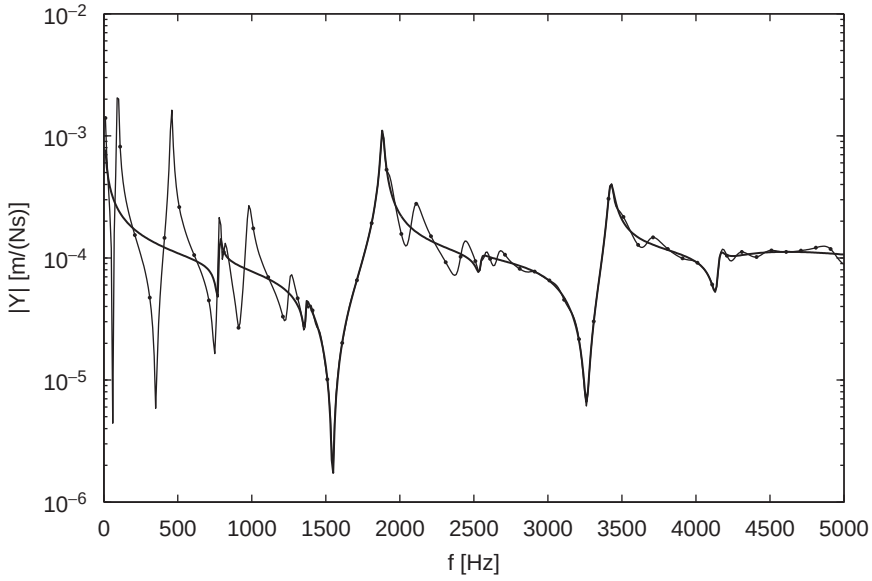

Fig. 5. Transfer mobility profile A, two subelements, free boundary: standard FE-results -•- and WFE-results–(bold) (resp. at $x = 0.1$ m, $y = 0$, $z = 0.1$ m).

excitation and response points. The maintained accuracy is demonstrated by calculating input and transfer mobilities for different number of included waves. Results are shown in Figs. 6–10.

The reduction from 792 characteristic waves (full) to 150, principal propagating waves ($|\lambda|$ closest to 1), gives satisfactory results in the complete investigated frequency range. As the nearfield in the vicinity of the excitation point is established by non-propagating waves, which are not fully taken into account in the reduced basis, there is an observable underestimation of the magnitude of the input mobility (Fig. 6).

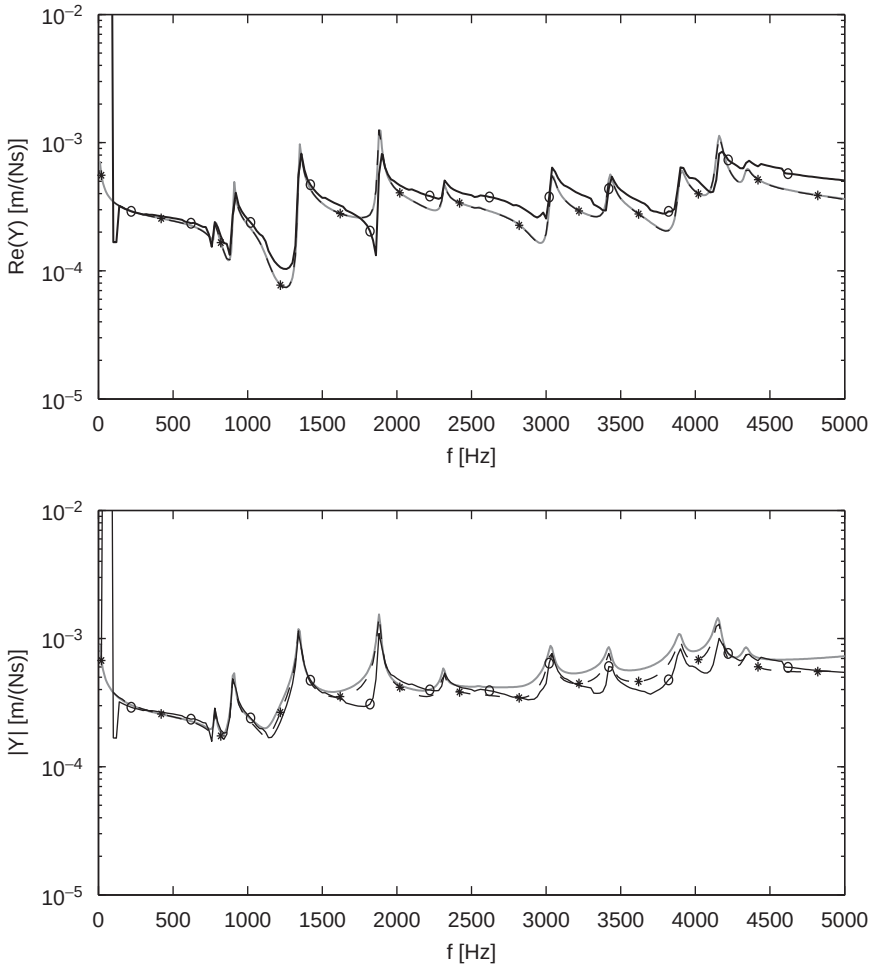

Fig. 6. Input mobility of profile A, two subelements, free boundary: influence of wave basis reduction on forced response (full: —(grey), 150 waves: – –*– – (black), 50 waves: –o– (black)).

A significant deviation can be observed also for the transfer mobilities to lateral points in the x-direction (Figs. 7 and 9).

For remote response positions the differences between full and moderately reduced wave basis are negligible, which is expected as these positions are only influenced by propagating waves.

The reduction to only 50 propagating waves suffers from stronger deviations, most pronounced in the vicinity of the excitation position where nearfields, i.e. decaying and complex waves, contribute significantly. The results become unreliable at some frequencies, where the strongly reduced wave basis is no longer an appropriate representation of the physics.

Overall, the reduced wave basis serves as an effective method to simplify forced response calculations with reliable results as long as the degree of reduction is moderate and nearfield effects are not of primary concern.

5. Dynamic reduction methods

The use of a limited wave basis reduces the calculation effort considerably. For large plate sections, of many lateral subelements, however, it is desirable to further reduce the system matrices of the eigenvalue problem. The idea is to use standard dynamic finite element reduction methods commonly used in FE-packages to reduce the calculation effort. Two methods are applied here, the Guyan or static reduction method [7] and the

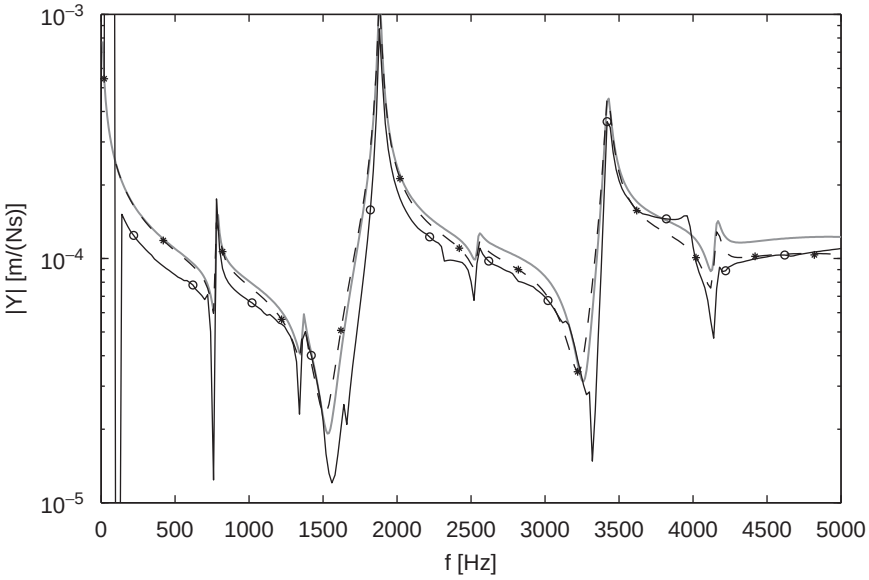

Fig. 7. Transfer mobility of profile A, two subelements, free boundary (response at $x = 0.1\,\mathrm{m}$, $y = 0$, $z = 0$): influence of wave basis reduction on forced response (full: —(grey), 150 waves: – –*– – (black), 50 waves: –o– (black)).

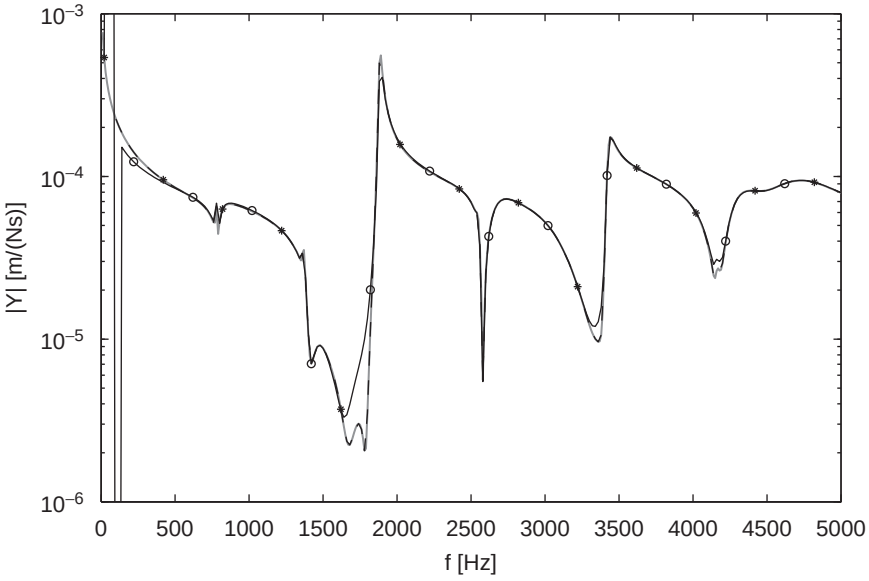

Fig. 8. Transfer mobility of profile A, two subelements, free boundary (response at $x = 0.1\,\mathrm{m}$, $y = 0$, $z = 0.5\,\mathrm{m}$): influence of wave basis reduction on forced response (full: —(grey), 150 waves: – –*– – (black), 50 waves: –o– (black)).

standard improved reduction system (IRS) [8]. In general, the IRS is more reliable, see e.g. Ref. [9], but the widely used Guyan reduction is also investigated. After performing the reduction scheme, the reduced mass and stiffness matrices, $\mathbf{M}_{\mathbf{red}}$ and $\mathbf{S}_{\mathbf{red}}$ respectively, are applied for the WFE wave basis evaluation as outlined in Ref. [1].

All the reduction methods eliminate some of the DOFs, the so called slave DOFs (index **s**). The remaining DOFs are called master DOFs (index **m**). For the reduction process the mass and stiffness matrices **M** and **S**

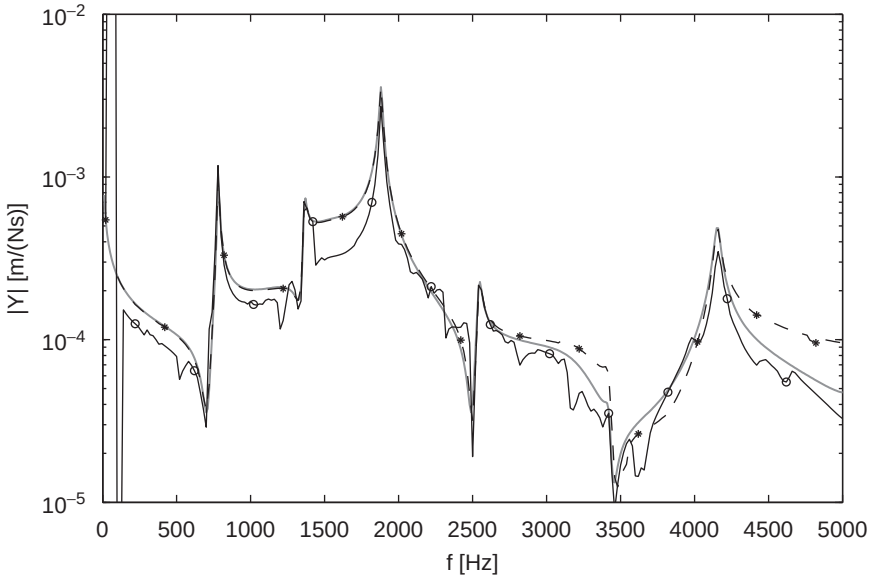

Fig. 9. Transfer mobility of profile A, two subelements, free boundary (response at $x = 0.1$, $y = 0.05$ m, $z = 0$): influence of wave basis reduction on forced response (full: —(grey), 150 waves: – –*– – (black), 50 waves: –o– (black)).

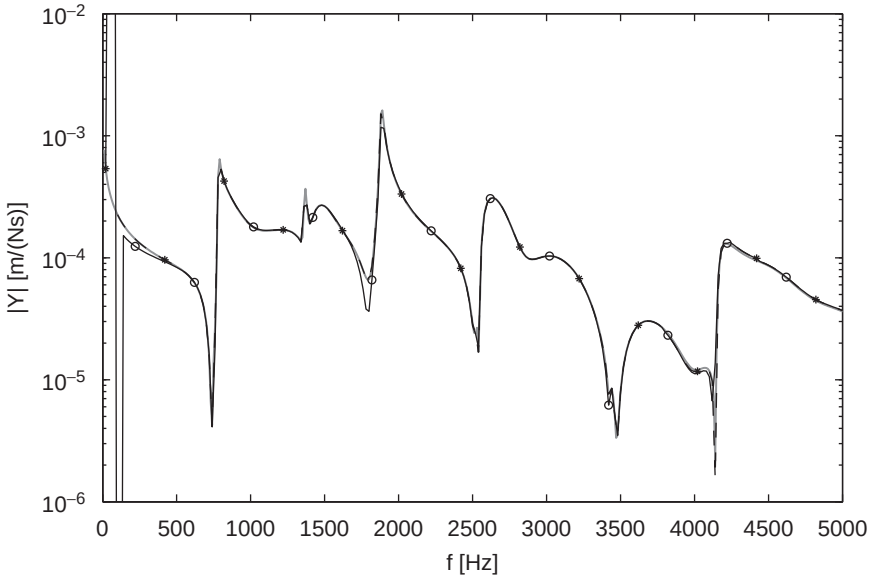

Fig. 10. Transfer mobility of profile A, two subelements, free boundary (response at $x = 0.1$, $y = 0.05$, $z = 0.5$ m): influence of wave basis reduction on forced response (full: —(grey), 150 waves: – –*– – (black), 50 waves: –o– (black)).

are partitioned in the following way:

$$\mathbf{M} = \begin{bmatrix} \mathbf{M}_{\mathbf{mm}} & \mathbf{M}_{\mathbf{ms}} \\ \mathbf{M}_{\mathbf{sm}} & \mathbf{M}_{\mathbf{ss}} \end{bmatrix}, \quad \mathbf{S} = \begin{bmatrix} \mathbf{S}_{\mathbf{mm}} & \mathbf{S}_{\mathbf{ms}} \\ \mathbf{S}_{\mathbf{sm}} & \mathbf{S}_{\mathbf{ss}} \end{bmatrix}. \tag{3}$$

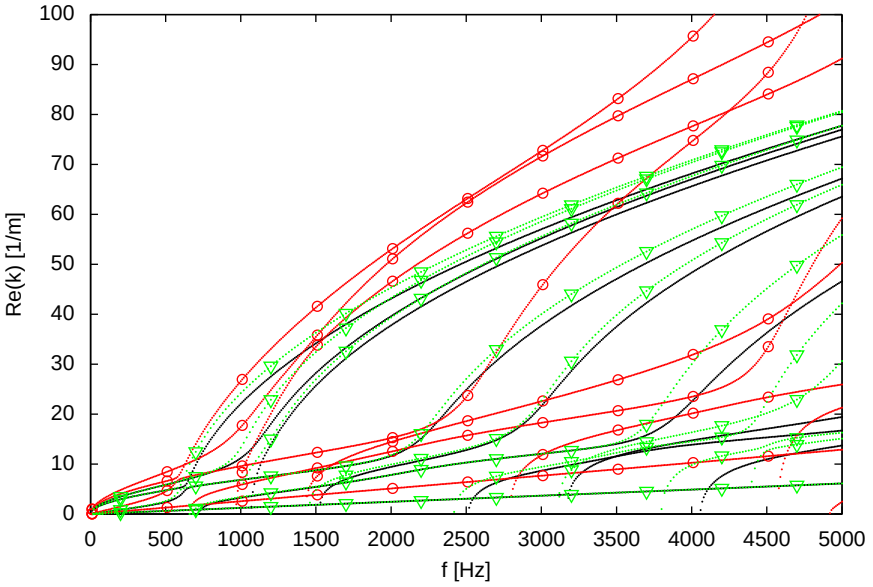

Fig. 11. Influence of mesh size and periodic length L_e on evaluated dispersion characteristics of profile A, single subelement in x-direction. No markers: 10 mm × 10 mm; o: 25 mm × 25 mm; ▽: 25 mm × 5 mm.

Depending on the reduction method, a reduction matrix $\mathbf{W}$ is defined and the reduced mass and stiffness matrices are calculated from

$$\mathbf{M_{red}} = \mathbf{W}^T\mathbf{M}\mathbf{W}, \quad \mathbf{S_{red}} = \mathbf{W}^T\mathbf{S}\mathbf{W}. \tag{4}$$

In the Guyan case the reduction matrix reads

$$\mathbf{W}_{Guyan} = \begin{bmatrix} \mathbf{I} \\ -\mathbf{S}_{\mathbf{ss}}^{-1}\mathbf{S}_{\mathbf{sm}} \end{bmatrix}. \tag{5}$$

This reduction neglects the inertia terms of the slave DOFs, which is a good approximation at low frequencies and is accurate in the static case, where inertia forces vanish.

The IRS method uses pseudo-static forces of the inertia terms at low frequencies and improves the Guyan reduction method in this way,[1]

$$\mathbf{W}_{IRS} = \mathbf{W}_{Guyan} + \begin{bmatrix} \mathbf{0} & \mathbf{0} \\ \mathbf{0} & \mathbf{S}_{\mathbf{ss}}^{-1} \end{bmatrix} \mathbf{M}\mathbf{W}_{Guyan}\mathbf{M}_{red,Guyan}^{-1}\mathbf{S}_{red,Guyan}. \tag{6}$$

5.1. Influence of dynamic reduction and mesh coarsening on dispersion characteristics

The reduction techniques described in the preceding section have to compete with mesh coarsening approaches, which similarly reduce the calculation effort. Therefore dispersion results for a single subelement and different mesh sizes are shown in Fig. 11. The coarse mesh with 25 mm edge length of the quadratic shell elements cannot capture the wave propagation mechanisms for frequencies higher than 100 Hz. Significant reduction of the calculation effort without a drastic decrease of the accuracy, can be achieved by keeping the coarse mesh length in the lateral direction of the cross section, but reducing the element length in the

[1]Due to the inversion of the reduced mass matrix, it has to be assured that all massless DOFs are eliminated. Otherwise the matrix is rank deficient and the reduction process fails.

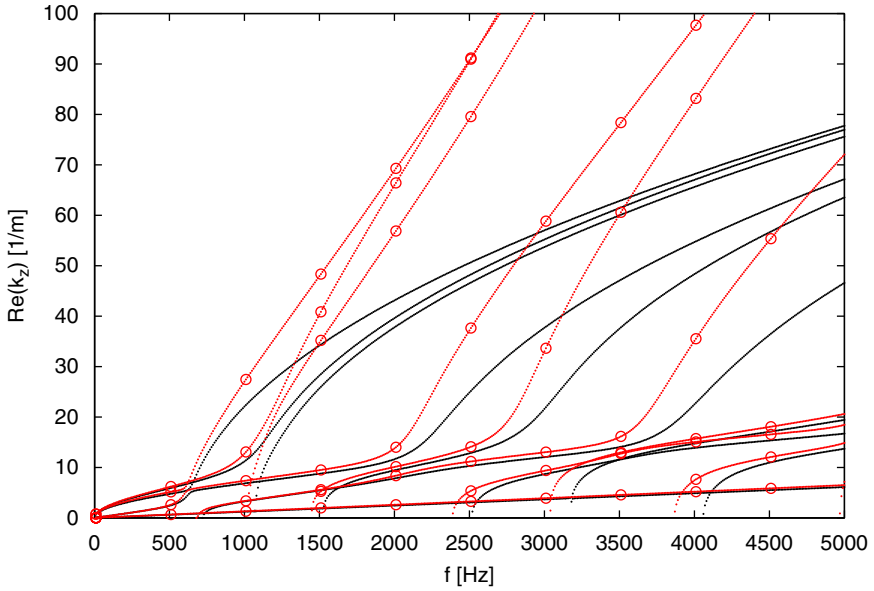

Fig. 12. Influence of Guyan reduction with all massless DOFs on evaluated dispersion characteristics of profile A, single subelement in x-direction. No markers: full calculation (10 mm × 10 mm); o: Guyan reduction (10 mm × 10 mm).

z-direction to 5 mm. In this case deviations are acceptable up to about 3000 Hz without an increase in the calculation effort. This insight is of major importance for practical applications of the method and supports the suggestions of Mead in Ref. [10] to use a small periodic length L_e.

The influence of Guyan reduction, using all massless DOFs, on dispersion characteristics, is illustrated in Fig. 12. It is obvious that the static reduction technique in this case fails to accurately represent the propagating waves with wavenumbers higher than $15\,\mathrm{m}^{-1}$. Figs. 11 and 12 show that in the global regime up to 500 Hz the Guyan reduction is more reliable than mesh coarsening.

The comparison of fine and coarse mesh or full and reduced model dispersion curves can serve as a means to identify the frequency/wavenumber limit for the applied reduction to cover the salient physics. Dispersion results for IRS are omitted for the sake of brevity.

5.2. Forced response using dynamic reduction

For the Guyan reduction method all massless (rotational) degrees of freedom are selected as slave DOFs for the presented results. For the IRS, half of the nodes are retained and additionally the massless DOFs are reduced, which is roughly a reduction to a quarter of the DOFs. The results are presented in Figs. 13–15.

Neither the Guyan reduced results nor the IRS results capture the mobilities of the full structure in an appropriate way. At very low frequencies, below the first cross sectional resonances, the static reduction is a reliable approximation. At higher frequencies the general trends are still appropriately represented by both methods, but there is a significant frequency shift to lower frequencies of about 10−20%, illustrating a de-stiffening effect. The results for the input mobility are more satisfying and give an acceptable representation compared with the reference mobility.

6. Calculated and measured mobility of train floor section

In this section, the forced response of a regional train floor section is investigated. The cross section of the extruded aluminium train floor is shown in Fig. 16. Normal force excitation is applied at the centre of the section, both at a stiffener position ($F_{stiffener}$) and at a plate field position ($F_{platefield}$). More details of the floor section are given in Refs. [1,11].

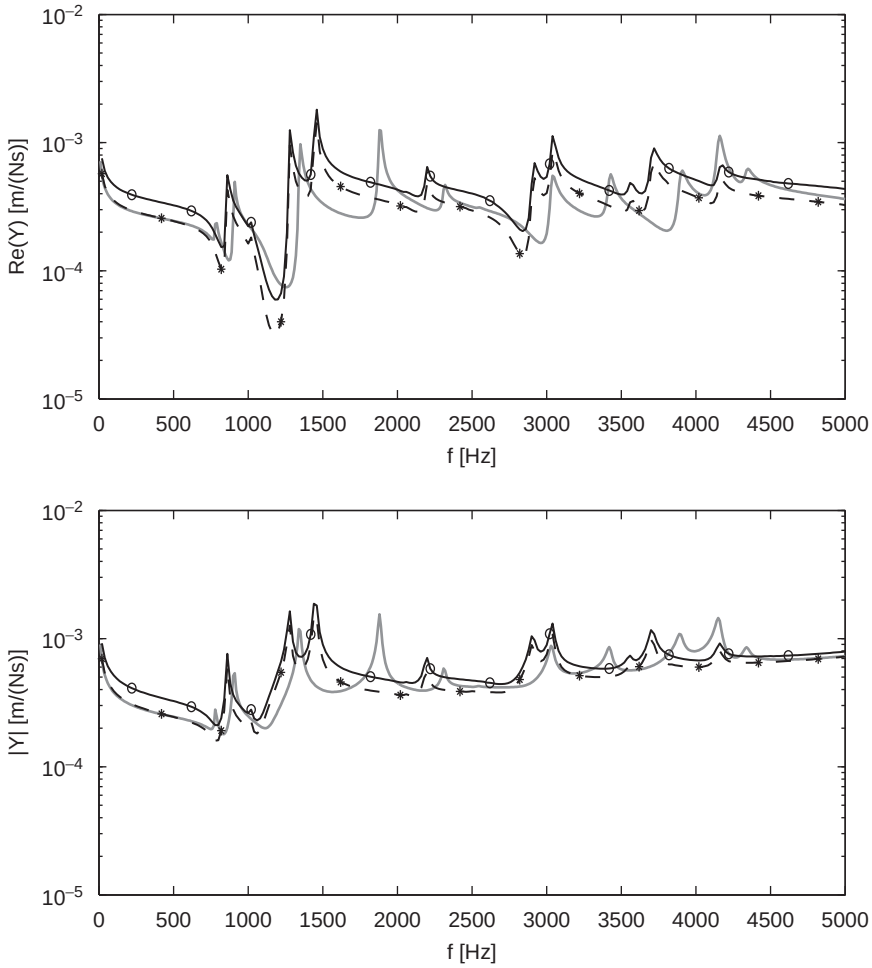

Fig. 13. Input mobility of profile A, two subelements, free boundary: influence of Guyan reduction and IRS (full (396 DOFs): —(grey), Guyan (198 DOFs): – –*– – (black), IRS (96 DOFs): –o– (black)).

For the case of plate field excitation, the measured and WFE-calculated input mobilities of the edge damped test section are shown in Fig. 17.[2]

The general trends of the calculated and measured input mobilities are a stiffness-like behaviour at frequencies below the first cut-on frequency of the strip for excitation at the centre of a plate strip. This is followed by a strong increase and a peak at the cut-on frequency at 340/400 Hz (calculated/measured). Up to the second cut-on frequency, accompanied by a second mobility peak, the behaviour is essentially beam-like. This is because the wave propagation is dominated by a one-dimensional propagation along the plate strip in the z-direction. The smaller peaks, between the cut-on frequencies in the test data, are caused by non-ideal anechoic terminations in the test set-up and are related to standing waves in the z-direction. Upon comparing the calculated and measured data, the shifts of the cut-on frequencies are related to the stiffening effect of the fillets at the joints of the extruded profile. This reduces the free width of the plate strip and constrains the edges, see Refs. [1,4].

For the force applied at a stiffener position, data of the damped test object is not available. Hence, the comparison is performed with test data of the freely suspended train floor section, which reveals its strong, resonant behaviour in this case. The strong resonant behaviour, induced by the finite length edge reflections,

[2]For practical reasons the acceleration could not be measured directly at the excitation point. The distance is about 1 cm and the measured mobility data are not phase calibrated, giving a decreasing real part at frequencies greater than 3000 Hz.

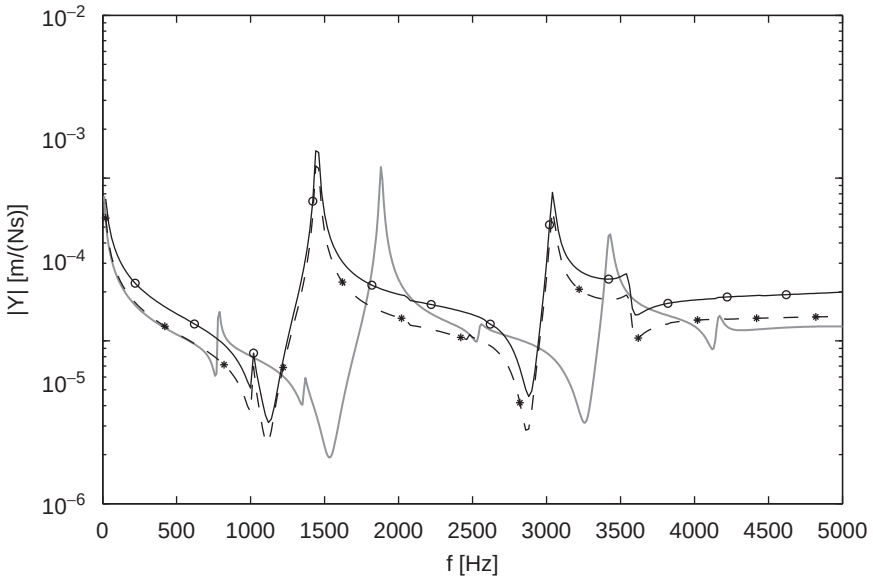

Fig. 14. Transfer mobility of profile A, two subelements, free boundary (response at $x = 0.1$ m, $y = 0$, $z = 0$): influence of Guyan reduction and IRS (full (396 DOFs): —(grey), Guyan (198 DOFs): – –*– – (black), IRS (96 DOFs): –o– (black)).

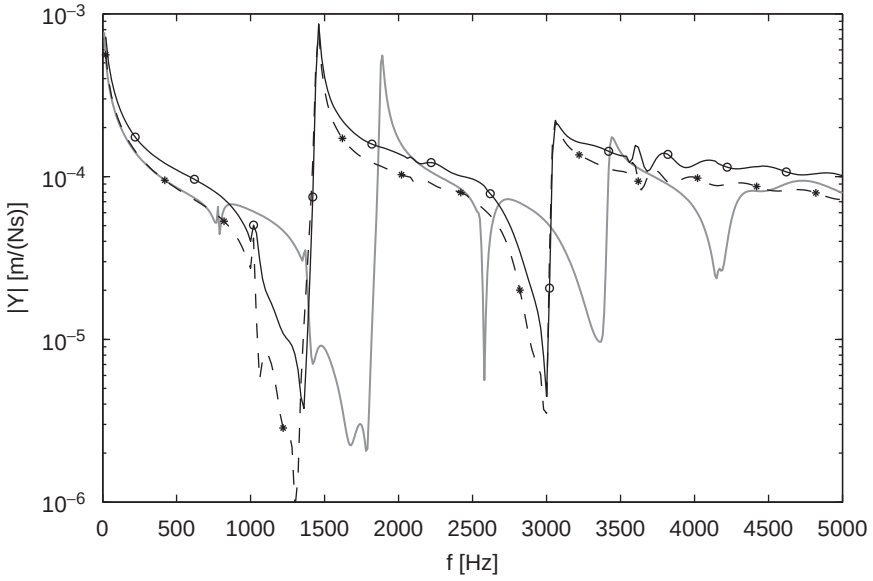

Fig. 15. Transfer mobility of profile A, two subelements, free boundary (response at $x = 0.1$ m, $y = 0$, $z = 0.5$ m): influence of Guyan reduction and IRS (full (396 DOFs): —(grey), Guyan (198 DOFs): – –*– – (black), IRS (96 DOFs): –o– (black)).

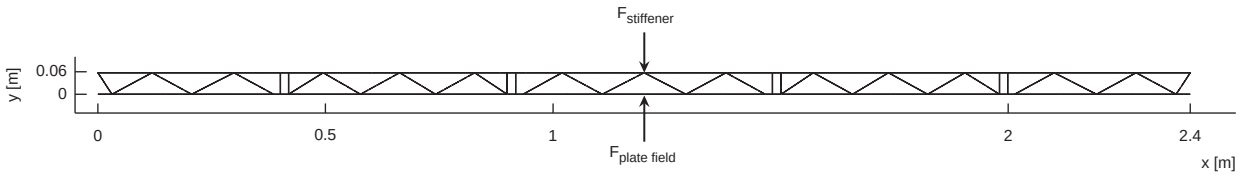

Fig. 16. Cross section and force excitation positions of investigated train floor section.

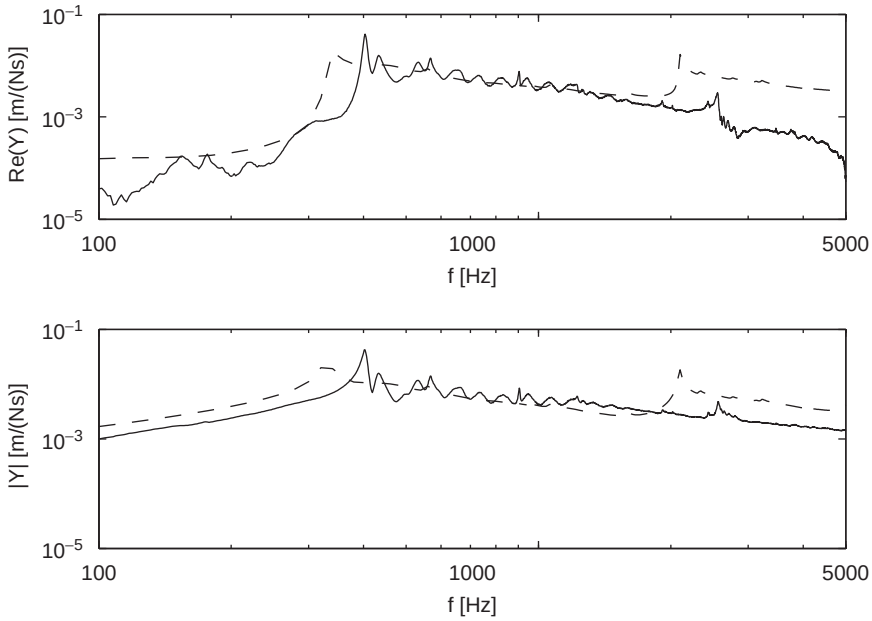

Fig. 17. Measured (—) and WFE-calculated (– –) input mobility of edge damped train floor section for normal force excitation at the centre position (plate field).

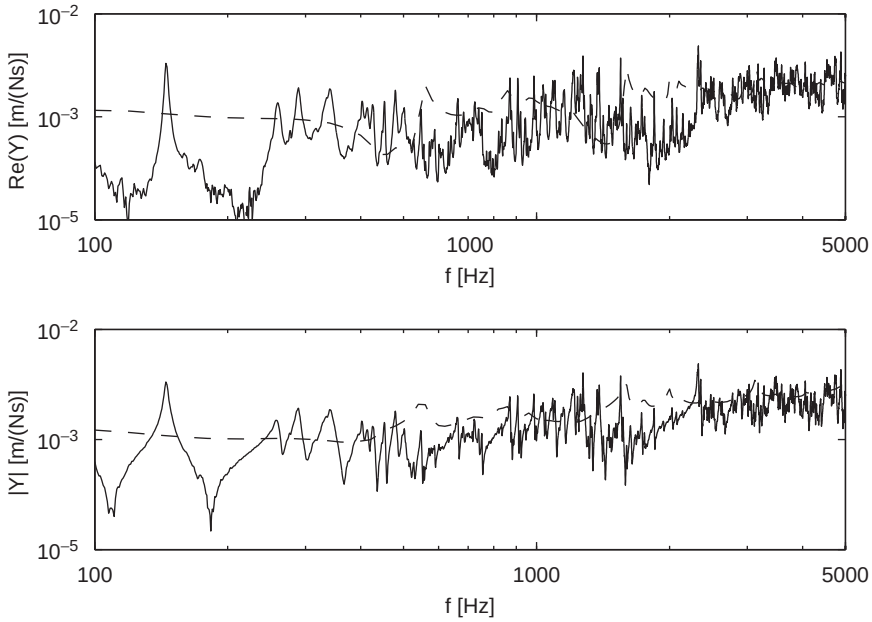

Fig. 18. Measured, freely suspended (—) and infinite WFE-calculated, edge damped (– –) input mobility of train floor section for normal force excitation at stiffener position at the centre of plate.

mainly in the z-direction, is clearly visible in Fig. 18. Following the mean value approach for infinite systems [12], the general trends of the measured input mobilities are captured by the WFE-calculation for this excitation case. Details of the test set-up with free boundary conditions and additional test results are reported in Ref. [11].

Though the similarity between calculation and measurement in this case is not obvious, general characteristics like alternating stop- and pass-band behaviour can be observed in both the real part and the magnitude. The frequency shifts between calculation and measurement is stronger than for the plate field excitation case. As expected, the mobility at a stiffener position is generally lower than at a plate field.

7. Concluding remarks

The forced response results, presented in this paper, demonstrate the capabilities of the WFE-calculations. This is done through a comparison with standard FE-calculations. The fact that the plate can be taken as infinite in longitudinal direction, without enlarging the computational effort, is especially valuable for a general profile design where otherwise longitudinal resonances would obscure the trends for arbitrary lengths. It is demonstrated that the application of a reduced wave basis can serve as a promising means to limit the necessary calculation effort for WFE applications, also comprising assessments of radiated sound to a fluid environment. Only if nearfield effects are of primary concern, the full wave basis has to be retained. The application of standard reduction methods like the Guyan or IRS is far less reliable and should be avoided. The train floor section demonstrates the applicability to industrial light weight profiles.

Acknowledgement

The funding of the German Research Foundation (DFG) within the project "Körperschall typischer Leichtbaustrukturen" (Pe 1155/3) is gratefully acknowledged.

References

[1] T. Kohrs, B.A.T. Petersson, Wave beaming and wave propagation in light weight plates with truss-like cores, *Journal of Sound and Vibration* (2008), doi:10.1016/j.jsv.2008.09.033, available online at 13 November.
[2] B.R. Mace, D. Duhamel, M.J. Brennan, L. Hinke, Finite element prediction of wave motion in structural waveguides, *Journal of Acoustical Society of America* 117 (5) (2005) 2835–2843.
[3] D.J. Thompson, Wheel-rail noise generation, III: rail vibration, *Journal of Sound and Vibration* 161 (3) (1993) 421–446.
[4] T. Kohrs, B.A.T. Petersson, Wave propagation in light weight profiles with truss-like cores: wavenumber content, forced response and influence of periodicity perturbations, *Journal of Sound and Vibration* 304 (3–5) (2007) 691–721.
[5] D. Duhamel, B.R. Mace, M.J. Brennan, Finite element analysis of the vibrations of waveguides and periodic structures, *Journal of Sound and Vibration* 294 (1–2) (2006) 205–220.
[6] Y. Waki, B.R. Mace, M.J. Brennan, Vibration analysis of a tyre mode using the wave finite element method, in: *19th International Congress on Acoustics*, Madrid, 2007.
[7] R.J. Guyan, Reduction of stiffness and mass matrices, *AIAA Journal* 3 (1965) 380.
[8] J. O'Callahan, A new procedure for an improved reduced system (IRS), in: *Seventh International Modal Analysis Conference*, Las Vegas, Nevada, February 1989.
[9] P.E. McGowan, A.F. Angelucci, M. Javeed, Dynamic test/analysis correlation using reduced analytical models, NASA Technical Memorandum 107671, Langley Research Center, Hampton, Virginia, September 1992.
[10] D. J. Mead, An introduction to FE-PST the combined use of finite element analysis and periodic structure theory, Technical Memorandum no. 959, Institute of Sound and Vibration Research, University of Southampton, March 2006.
[11] T. Kohrs, Wave propagation in light weight plates with truss-like cores, Doctorate Thesis, Institute of Fluid Mechanics and Engineering Acoustics, Technische Universität Berlin, Germany, 2008.
[12] E. Skudrzyk, The mean-value method of predicting the dynamic response of complex vibrators, *Journal of the Acoustical Society of America* 67 (4) (1980) 1105–1135.